Cerebral Cortex, November 2017;27: 5343–5352

doi: 10.1093/cercor/bhx219
Advance Access Publication Date: 28 August 2017
Original Article

ORIGINAL ARTICLE

Neural Substrate for Metacognitive Accuracy of Tactile Working Memory

Juha Gogulski[1,2], Rasmus Zetter[2], Mikko Nyrhinen[1,2,3], Antti Pertovaara[1] and Synnöve Carlson[1,2,3]

[1]Department of Physiology, Faculty of Medicine, University of Helsinki, Helsinki 00014, Finland, [2]Department of Neuroscience and Biomedical Engineering, Aalto University School of Science, Aalto 00076, Finland and [3]Aalto TMS Laboratory, Aalto NeuroImaging, Aalto University, Aalto 00076, Finland

Address correspondence to Juha Gogulski and Synnöve Carlson. Email: juha.gogulski@helsinki.fi (J.G.); synnove.carlson@aalto.fi (S.C.).

Juha Gogulski and Rasmus Zetter share the first authorship

Abstract

The human prefrontal cortex (PFC) has been shown to be important for metacognition, the capacity to monitor and control one's own cognitive processes. Here we dissected the neural architecture of somatosensory metacognition using navigated single-pulse transcranial magnetic stimulation (TMS) to modulate tactile working memory (WM) processing. We asked subjects to perform tactile WM tasks and to give a confidence rating for their performance after each trial. We circumvented the challenge of interindividual variability in functional brain anatomy by applying TMS to two PFC areas that, according to tractography, were neurally connected with the primary somatosensory cortex (S1): one area in the superior frontal gyrus (SFG), another in the middle frontal gyrus (MFG). These two PFC locations and a control cortical area were stimulated during both spatial and temporal tactile WM tasks. We found that tractography-guided TMS of the SFG area selectively enhanced metacognitive accuracy of tactile temporal, but not spatial WM. Stimulation of the MFG area that was also neurally connected with the S1 had no such effect on metacognitive accuracy of either the temporal or spatial tactile WM. Our findings provide causal evidence that the PFC contains distinct neuroanatomical substrates for introspective accuracy of tactile WM.

Key words: metacognition, TMS, tractography, working memory

Introduction

The prefrontal cortex (PFC) is known to be involved in executive functions, attention, and working memory (WM). More recently, it has been shown to have a role also in metacognition (Fleming and Dolan 2012), an ability of human subjects to introspectively monitor and control their own cognitive processes (Nelson and Narens 1990). Failure of this ability can be observed in many neuropsychiatric disorders, for example in schizophrenia, Alzheimer's disease and traumatic brain injury (David et al. 2012). Robust, confound-free quantitative measures of metacognition have only recently been developed (Maniscalco and Lau 2012; Overgaard 2015), and the underlying, distinct neural frameworks remain poorly understood. Lesion and neuroimaging studies have suggested that the PFC is crucial for metacognitive ability (Fleming et al. 2010; Fleming and Dolan 2012). The lateral parts of the PFC (Chua et al. 2014) and the frontopolar cortex (Yokoyama et al. 2010) have been linked with accuracy in retrospective confidence judgments. Studies applying transcranial magnetic stimulation (TMS) have also reported a relationship between metacognition and the PFC.

Metacognition was impaired in visual perception tasks by repetitive TMS to the dorsolateral PFC (Rounis et al. 2010), and improved by fMRI-guided TMS to the most anterior parts of the PFC (Rahnev et al. 2016). Moreover, perturbation of the premotor cortex with single-pulse TMS reduced metacognitive confidence in visual discrimination tasks (Fleming et al. 2015). While metacognition has been studied using various kinds of auditory and visual tasks, only a few studies have employed tactile tasks (Whitmarsh et al. 2014, 2017).

The PFC integrates information from different sensory modalities and supports diverse higher cognitive processes including perception, memory, and metacognition. It is still unclear, however, how the different sensory modalities (visual, auditory, and somatosensory) and attributes of stimuli are represented in the PFC during the different cognitive processes. The involvement of the PFC in WM, a brain mechanism that enables temporary storage and manipulation of information (Baddeley 1992), has been extensively studied (D'Esposito and Postle 2015). Influential models have been put forward about the functional organization of WM in the PFC. One model presents that the functional organization of WM in PFC is based on the type of stimuli that are kept in memory (Goldman-Rakic 1995). This model suggests that the dorsolateral PFC regions are more involved in WM processing of the spatial properties of the stimuli and the ventrolateral PFC areas in non-spatial properties of the stimuli (Wilson et al. 1993; Romanski et al. 1999). The functional organization of the PFC has also been suggested to be based on the type of processes involved in WM such as monitoring events, manipulating and maintaining information in WM (Petrides 2005). Most WM studies have applied visual or auditory stimuli as memoranda. Although tactile WM has been studied much less than visual or auditory WM, these studies have shown that keeping the properties of tactile stimuli in WM also activates distinct PFC areas (Romo et al. 1999; Gruber et al. 2000; Romo and Salinas 2003; Stoeckel et al. 2003; Numminen et al. 2004; Preuschhof et al. 2006; Kaas et al. 2007; Kostopoulos et al. 2007).

Interindividual differences in both brain structure and function (Penfield and Boldrey 1937; Zilles et al. 1997) present a challenge in neuroscience, as the use of normalization and group-level analyses can mask otherwise evident findings (Kanai and Rees 2011). This challenge is most apparent in the evolutionarily young frontal areas (Mueller et al. 2013) that are involved in higher cognitive functions such as WM and metacognition. Modern, non-invasive brain imaging methods, including diffusion-weighted magnetic resonance imaging (dw-MRI), have provided promising means to correlate structural variability with differences in various cognitive domains; visuomotor processing (Budisavljevic et al. 2016), visual WM (Golestani et al. 2014) and metacognitive accuracy (Fleming et al. 2010). As the PFC covers a large cortical area in humans, it is difficult to find a relevant TMS stimulation site that would also be functionally comparable between subjects. This challenge can be overcome by using different brain imaging methods that together enable investigating the neuronal underpinnings of cognitive processes despite interindividual topographical variability in brain structure and function.

In the PFC, both the superior (SFG) and middle (MFG) frontal gyri have been shown to be activated in vibrotactile frequency discrimination tasks involving WM, in which the subjects were instructed to remember and compare subsequent vibration frequencies (Pleger et al. 2006; Preuschhof et al. 2006). Moreover, an area in the MFG that had neural connections with the S1, was shown to be involved in tactile WM tasks where subjects memorized short temporal intervals of tactile paired pulses (Hannula et al. 2010). In a recent magnetoencephalography (MEG) study (Whitmarsh et al. 2017), alpha power of the SFG was shown to negatively correlate with metacognitive attention ratings in a tactile temporal discrimination task. In the current study, we investigated whether the areas of the MFG or SFG that are neurally connected with the S1, might also be involved in introspection of tactile *temporal* (comparison of time intervals) or *spatial* (comparison of spatial patterns) WM performance. Earlier neuroanatomical primate studies have shown that the PFC has neural connections with the primary somatosensory cortex (S1) (Preuss and Goldman-Rakic 1989). In humans, neural tracts between the PFC and S1 can be non-invasively determined by using probabilistic tractography based on dw-MRI. Such tractography-informed areas of the PFC have been shown to be involved in neural circuitries controlling tactile perceptual and WM processing (Hannula et al. 2010; Gogulski et al. 2015). The use of 2 types of tactile WM tasks allowed us also to test the hypothesis that the functional organization of metacognition might be based on the type of information that is kept in WM (here tactile spatial or non-spatial (i.e., temporal) information), resembling the organization of visual and auditory information processing in WM.

We designed an experimental paradigm, in which tactile WM of 2 different types of memoranda (temporal and spatial) can be studied with identical stimuli simply by changing the instructions to the subject. In both tasks, one trial consisted of two pin-pair stimuli. In the temporal WM task, the subjects were instructed to compare the time intervals of the two pin-pairs. In the spatial WM task, the subjects compared the spatial patterns of the two pin-pairs. We explored the functional neuroanatomy of metacognition by using these 2 types of WM tasks and individually tailored, tractography-guided TMS. We applied TMS to 2 locations in the PFC that had neural connections with the S1 (one area in the MFG and one in SFG), and investigated whether these areas of the PFC might also be involved in introspective judgments of tactile WM performance. The subjects' confidence ratings were used to estimate the metacognitive accuracy in each task and stimulation site (Maniscalco and Lau 2012).

Methods

Subjects

Altogether 15 healthy, right-handed volunteers (8 males and 7 females, age range 24–37 years, average age 29 years) with no history of neurological or psychiatric disorders participated in the study. The experimental design took into consideration the code of ethics as defined in the World Medical Association's Declaration of Helsinki, and the study was approved by the Aalto University Ethics Committee. Informed consent was obtained from all participants. Data from one subject were excluded from the analyses due to misunderstanding of the instructions; after performing the experiment, the subject reported that he always responded with the highest confidence level if he felt that there was not enough time to respond (this in spite of the fact that the experiment was self-paced). Thus, 14 subjects were left in the analyses.

Tactile Stimulator

Mechanical tactile stimuli were applied to the fingertip of the right index finger using a stimulator unit (Metec AG) originally designed for Braille reading, which was driven by a custom-

made control system. The stimulator has 8 rounded plastic pins (1.25 mm diameter, 2.5 mm spacing) organized in 2 rows which can be raised to a height of 0.7 mm with a rise time of 24 ms, generating a force of 0.17 N. Subjects were instructed to rest the fingertip of their right index finger on the stimulator with their hand positioned so that only the stimulated finger touched the stimulator device.

Structural and Diffusion-weighted MRI

Structural and dw-MR images were acquired using a 3 T MAGNETOM Skyra whole-body scanner (Siemens Healthcare) and a 32-channel receiving head coil. All subjects wore earplugs and tightly packed foam covers over their ears for additional hearing protection and to minimize head movement. A T1-weighted 3D-MPRAGE structural image was acquired using the following parameters: TR 2530 ms, TE 3.3 ms, TI 1100 ms, FA of 7°, in-plane FOV 256 × 256 mm, 1 mm isotropic voxels, 176 contiguous slices and a GRAPPA factor of 2. Diffusion-weighted images were acquired using a spin-echo echo-planar sequence with the following parameters: TR 9700 ms, TE 81 ms, bandwidth of 1436 Hz/px, echo spacing 0.78 ms, in-plane FOV 240 × 240 mm, 2 mm isotropic voxels, 65 contiguous axial slices and a GRAPPA factor of 2. The diffusion imaging scheme consisted of 64 non-collinear diffusion-sensitizing gradient orientations (b = 1000 s/mm^2) evenly distributed on a sphere. Several nondiffusion-weighted (b = 0 s/mm^2, b0) images were also acquired, including 7 images with phase encoding in the anterior–posterior direction and 6 images in the posterior–anterior direction.

For 5 subjects, previously acquired structural and dw-MRI data were utilized. For details related to the acquisition parameters, see Gogulski et al. (2015).

Processing of Diffusion-weighted MRI Data

To avoid high-frequency artifacts, the raw k-space dw-MRI data were filtered using a low-pass Hamming filter (implemented in Siemens' *syngo MR D13C* software, "medium" setting) before reconstruction. Processing of dw-MRI data was performed using the FSL software package developed at the Oxford Centre for Functional MRI of the Brain (Woolrich et al. 2009; Jenkinson et al. 2012). To minimize geometric distortions induced by susceptibility effects, b0 data were collected with two opposite phase encoding directions, resulting in pairs of images with distortions going in opposite directions. Using these pairs, the susceptibility-induced off-resonance field was estimated using a method similar to that described by Andersson et al. (2003), as implemented in the *topup* tool of FSL (Smith et al. 2004), and the 2 image sets were combined into a single distortion-corrected one. The same distortion correction was applied to the diffusion-weighted images. Motion and eddy current artifacts were retrospectively estimated and corrected using the *EDDY* tool of FSL (Andersson and Sotiropoulos 2016), which also takes into account the off-resonance field as estimated by *topup*. Bayesian estimation of diffusion parameters under a "ball-and-sticks" model was performed using the *BEDPOSTX* tool of FSL (Behrens et al. 2003, 2007; Hernández et al. 2013). To account for crossing fibers present in a large part of white matter, up to 2 fibers ("sticks") were assumed for each voxel.

Processing of the previously acquired MRI data was similar to the treatment presented here, although *topup* and *EDDY* could not be applied due to the lack of opposite phase encodings. Instead, eddy current correction was applied using the *eddy_correct* tool of FSL. Furthermore, no low-pass filtering was applied to these data. Otherwise, the processing was identical.

Transcranial Magnetic Stimulation Procedure

TMS sessions were conducted at the Aalto TMS laboratory (Aalto NeuroImaging, Aalto University) using a Magstim 200^2 monophasic stimulator unit (Magstim Co.) with a 70 mm figure-of-eight coil and Visor2 neuronavigation system (ANT Neuro).

For resting motor threshold (RMT) determination, we first identified the right abductor pollicis brevis (APB) representation on the left primary motor cortex (M1). This was done by orienting the TMS coil so that the induced electric field pointed anteriorly in relation to the central sulcus, perpendicular to the precentral gyrus. Motor evoked potentials from the APB were recorded using a NeurOne (Mega Electronics Ltd) electromyography (EMG) device and Ag-AgCl skin electrodes (Spes Medica Srl.). The M1 site that produced the largest motor response was identified as the APB representation on the M1 whereafter this location was used for RMT determination. The lowest TMS intensity at which ≥5 out of 10 stimuli produced a ≥50 μV peak-to-peak response in the EMG signal was defined as the RMT.

Determination of the Somatotopic Representation Area

After RMT determination, an individual tactile threshold curve was assessed using a single pin of the tactile stimulator. Eight blocks of 6 trials were delivered to the fingertip of the subject's right index finger. Five trials in each block included tactile stimuli with varying amplitudes and one trial had a sham stimulus. The trials were presented in random order.

During determination of the tactile threshold curve, a TMS pulse with an intensity of 50% of the maximum stimulator output was applied 20 ms after the onset of the tactile stimulus with the coil in the air (approximately 10 cm above the head of the participant). TMS was applied in the air to mimic the real S1 stimulation (see the next paragraph). In the sham condition, the TMS pulse was delivered without a tactile stimulus. The rise times, and thus amplitudes, of the 5 tactile stimuli were spaced apart by 0.3 ms (approximately 10 μm rise height if the rise velocity is assumed constant). The tactile stimulus amplitude which was felt in 90% of the trials was used for the remainder of the somatotopic blocking experiment.

To determine the somatotopic representation area of the fingertip of the right index finger, we started to explore the S1 by turning the TMS coil 180° from the orientation of the M1 stimulation location during RMT measurement. Tactile stimuli accompanied with a TMS pulse were applied, each trial consisting of a single pin being raised and a TMS pulse. Based on a previous study by our group (Hannula et al. 2005), navigated TMS was applied 20 ms after the onset of the tactile stimulus. The subjects were instructed to press the left button of a computer mouse held in their left hand if they perceived the tactile stimulus, and the right mouse button if they did not perceive the test stimulus. Subjects also answered verbally. If TMS of the initial S1 location did not block the tactile sensation, we moved the coil approximately 5 mm and repeated the procedure. The cortical location, where TMS blocked the perception of >50% of the tactile stimuli, was defined as the S1 hotspot ($S1_{HS}$). Determination of the RMT, tactile threshold and $S1_{HS}$ were performed in a separate session before the WM experiments.

Tractography

Connections between the $S1_{HS}$ and the SFG as well as the MFG were probed using probabilistic tractography as implemented in the *probtrackx* tool of FSL (Behrens et al. 2003). After functional determination of the $S1_{HS}$, its location was transferred to the anatomical T1 image and registered to the diffusion space. A region around the $S1_{HS}$ coordinates with an average volume of 81 voxels (SEM 6 mm), was selected as a 3D seed mask for tractography. Tracts were generated starting from the seed mask (step length = 0.5 mm; maximum number of steps = 2000; number of samples = 5000; curvature threshold = 0.2), which resulted in each voxel attaining a connectivity value corresponding to the number of probabilistic streamlines passing through the voxel and the seed region. The connectivity threshold was set on an individual basis to find the most credible connection with the MFG and SFG. The termination points of these connections were designated as the MFG_{HS} and SFG_{HS}, respectively. Care was taken not to lower the connectivity threshold to such a level that nonspecific connections across the brain were observed (average threshold for MFG_{HS} was 114 [SEM 21], and for SFG_{HS} 52 [SEM 9]).

For visualization of the tract seed- and termination points, single-voxel masks were drawn in the center of the $S1_{HS}$, MFG_{HS}, and SFG_{HS}. The masks were then transformed to the MNI space using a nonlinear deformation algorithm implemented in SPM12 (http://www.fil.ion.ucl.ac.uk/spm/). Finally, visualization was performed using pysurfer (https://pysurfer.github.io/) to project the points to the closest surface point on the pial surface in the *fsaverage* template of Freesurfer (http://freesurfer.net/) (Fig. 1c). To correct for errors introduced in the normalization process causing some points to be projected across sulci, small manual corrections were applied to 5 of the visualized points (see Supplementary Material, Table S1). Individual tractography visualizations are shown in Figure 1b and in the Supplementary Material (Fig. S3).

Transcranial Magnetic Stimulation During the Working Memory Tasks

During the WM tasks, single-pulse TMS was applied at 110% of the RMT except for 3 subjects, for which the intensity had to be lowered to 100% (2 subjects) and to 95% (one subject) due to uncomfortable scalp sensations. In each trial, a single time-locked TMS pulse was delivered during the delay period (the period between the two pin-pairs, Fig. 2a). Based on our earlier studies, the TMS was applied at a time point (300 ms from the start of the delay period) that has been found to modulate WM performance (Hannula et al. 2010; Savolainen et al. 2011). TMS was applied either to the MFG_{HS}, the SFG_{HS} or to a midline control site (vertex) located at the Pz electrode position of the 10–20 electroencephalography (EEG) electrode positioning system. When stimulating the MFG_{HS} or the SFG_{HS}, the coil was oriented so that the induced electric field pointed perpendicularly to the gyral wall. When TMS was applied to the vertex, the coil was oriented so that the induced electric field was directed caudally. The delivery of the tactile stimuli and the TMS pulses was controlled using Presentation software (Neurobehavioral Systems) which also logged the responses of the subjects.

Working Memory Tasks

Temporal and spatial aspects of tactile WM were studied in 2 separate tasks that had identical stimuli (Fig. 2). This experimental design allowed us to study both spatial and temporal

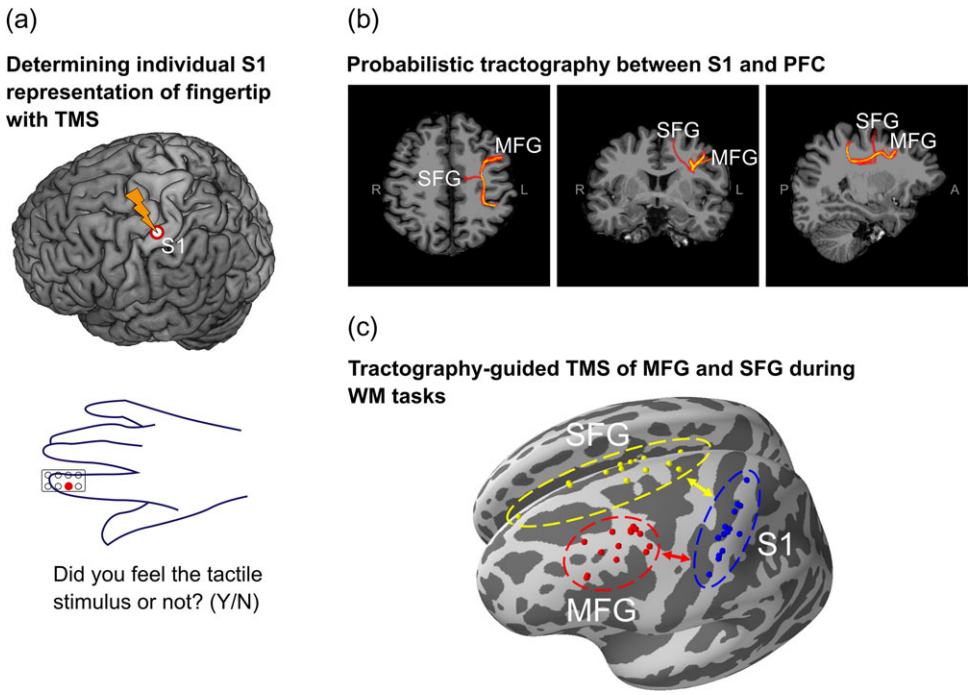

Figure 1. Determination of TMS targets on the PFC. (*a*) Somatotopic representation area of each subject's fingertip was determined by blocking the tactile sensation with TMS. (*b*) The S1 blocking site was used as a seed point for tractography. The illustration represents an intensity projection example of one subject's probabilistic tractography result between S1 and PFC, overlaid on an anatomical MRI. The sagittal, coronal, and axial slices were chosen to demonstrate the course of the tracts between the S1 and the 2 locations on the PFC (MFG and SFG). Other individual tractography visualizations are presented in the Supplementary Material (Fig. S2). (*c*) Interindividual variability of PFC-S1 tracts visualized on the inflated surface of a normalized template brain. Yellow spheres represent tract ending points in the SFG, red spheres indicate tract endings in the MFG. Each TMS target was chosen on the basis of individual anatomical fiber tracts. Blue spheres represent tractography seed points, i.e., the S1 representation areas of each subject's fingertip ($n = 14$).

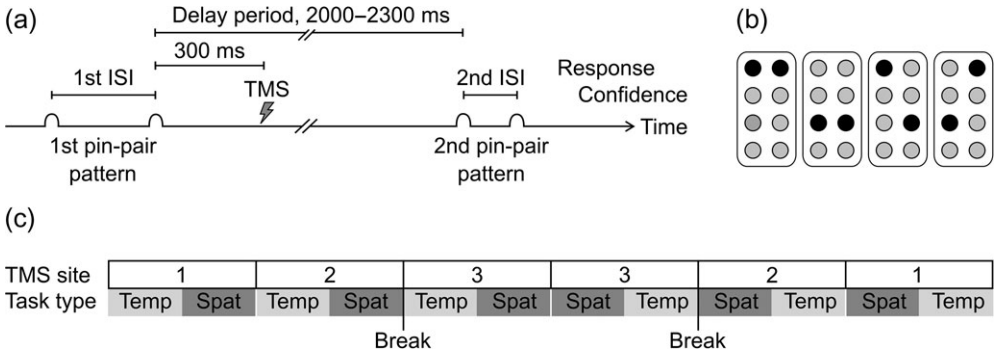

Figure 2. Experimental setup. (*a*) Illustration of the timeline of one example trial. A single TMS pulse was applied 300 ms after the first pin-pair (after the start of the delay period). (*b*) The 4 possible pin-pair patterns, with dark circles representing raised pins and light gray circles representing unused pins. (*c*) Time-flow of the WM experiment, showing the counterbalancing of the 2 task types and the 3 TMS sites (numbers 1–3 refer to MFG, SFG, and control sites). The order of the TMS sites was counterbalanced within and across subjects. The order of the WM tasks was counterbalanced within subjects. Temp = temporal WM task, Spat = spatial WM task.

tactile WM without any stimulus-related confounds. The memoranda in the tasks were two sequential, clearly perceivable pin-pairs that were presented with an interval of 2000–2300 ms (the delay period, Fig. 2*a*). The delay period was kept relatively short so that the experiment would not become too long while still providing as many trials as possible. The duration of the delay period applied here (in the order of a few seconds) is typical for WM tasks in experimental situations (Goldman-Rakic 1995). Each pin-pair consisted of a single pin being raised followed by a second pin being raised after a specified interstimulus interval (ISI) of 120–430 ms. Subjects were seated in front of a computer screen, on which instructions were shown. Subjects were instructed to visually fixate on a small cross centered on the screen when no instructions were displayed.

In the temporal WM task, the subjects were instructed to press the left button of a computer mouse held in their left hand if the ISIs of the two pin-pairs were the same, and the right button if they were different. In the spatial WM task, the subjects pressed the left button if the patterns of the two pin-pairs were the same, and the right button if they were different. Apart from the response instructions, the stimulus parameters were identical in the 2 tasks. There was no explicit limit to the response time, but the subjects were instructed to respond as quickly and accurately as possible after each trial (i.e., after two pin-pairs). Subjects also reported their answer verbally and gave a confidence rating after their response on a 3-level scale (3 = sure, 2 = unsure, and 1 = guess). The intertrial interval, measured from the response, was 2500 ms.

In the beginning of the WM experiment, the subjects performed two short practice rounds of both the spatial and temporal WM tasks. In the practice rounds, the TMS coil was held in the air approximately 10 cm above the head of the subject. If the performance level was ≥70% correct responses, we proceeded to the real experiment, if not, more practice rounds were conducted until a performance level of ≥70% correct responses was reached.

One task block included 18 trials, and blocks of either task type were presented 6 times (Fig. 2*c*). In half of the trials in a block, the spatial patterns (Fig. 2*b*) of the two pin-pairs were different. In the same manner, the first ISI in half of the trials in a block was 260 ms and in the other half 290 ms, and in half of the trials in a block the second ISI was 140 ms longer or shorter (randomized). The ISIs were chosen based on preliminary behavioral testing (see the Supplementary Material and Fig. S1). The order of the task types was counterbalanced within subjects, and the order of the TMS sites was counterbalanced both within and across subjects (Fig. 2*c*). Two short breaks were taken during the experiment to minimize subject fatigue. To assess the level of alertness of the subjects, the subjects were asked to report their alertness level on a 5-level scale (1 = sleepy, 5 = alert) before the beginning of each block. In case they were sleepy, a short extra break was taken.

Bootstrap Statistical Analysis of Metacognitive Accuracy

Metacognitive (type 2) sensitivity, i.e., the subjects' ability to introspectively judge their own performance, was analyzed using the signal detection theory (SDT)-based meta-*d*' metric (Maniscalco and Lau 2012) which is expressed in the same units as the type 1 sensitivity (task performance) metric *d*'. To avoid any influence of type 1 sensitivity on the type 2 analysis, type 2 sensitivity in relation to type 1 sensitivity was used by subtracting type 1 *d*' from the meta-*d*' value (Fleming and Lau 2014). Meta-*d*' – *d*' values measure metacognitive accuracy; a value of 0 indicates a so-called ideal observer with performance in line with type 1 SDT, whereas a meta-*d*' – *d*' < 0 indicates metacognitive performance worse than expected by type 1 SDT. With the present dataset, subject-per-subject analysis could lead to unstable estimates of meta-*d*' – *d*' because of the relatively low number of trials per subject (Barrett et al. 2013). Therefore, we employed a sampling-based bootstrap statistical analysis (Mooney and Duval 1993) in which data from all subjects were pooled together, as described earlier (Fleming et al. 2014; Maniscalco and Lau 2015). 100 000 bootstrap samples were drawn with replacement for each task- and stimulation site combination, whereafter the resulting bootstrap sample distributions were compared through the use of 95% confidence intervals (Fig. 3). Additionally, we calculated response-specific meta-*d*' – *d*' bootstrap distributions for the "same" and "different" responses (see Supplementary Fig. S5 and Table S2) and HMeta-d (Fleming 2017) for both tasks and stimulation sites (see Supplementary Fig. S6 and Table S3). The bootstrap distributions were visualized using R software (http://www.R-project.org/) and the ggplot2 – package (http://ggplot2.org/). Meta-*d*' was fit to the data by a maximum likelihood estimation procedure using MATLAB code available at http://www.columbia.edu/~bsm2105/type2sdt/.

Behavioral Data Analysis

Due to the small number of trials with the lowest confidence level ("guess", 87 trials in the entire dataset across all subjects),

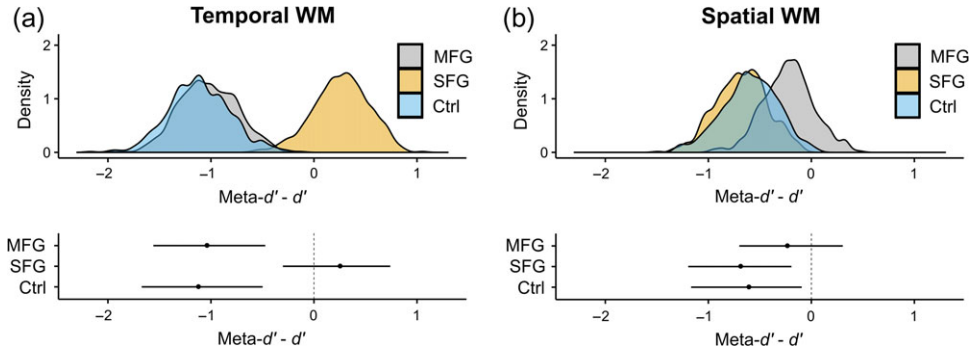

Figure 3. Effect of TMS on metacognitive accuracy. (*a*) TMS of the SFG enhanced metacognitive accuracy of temporal WM task. (*b*) In the spatial WM task, TMS did not have a significant effect on metacognitive accuracy. Density plots (above) and 95% confidence intervals (below) consist of 100 K bootstrap samples (n = 14). Ctrl = control site.

only the two higher confidence levels (labeled "High" and "Low" in the results) were included in all analyses of the behavioral data.

The percentage of correct responses was used as an index of task performance (Fig. 4*a*,*b*). The responses were grouped into high confidence and low confidence categories in each task and stimulation site (Lee et al. 2013). Statistical analyses of the task performance were conducted with two separate two-way repeated-measures analyses of variance (rmANOVA; factors: confidence and stimulation site), one for the temporal and another for the spatial WM task. The differences in overall performances between the two tasks were analyzed using *t*-tests with Bonferroni multiple comparisons correction. Response times were analyzed similarly as the task performance (see Supplementary Fig. S4), using two separate two-way rmANOVAs for each WM task (factors: confidence and stimulation site).

The proportions of responses rated as "high confidence" (i.e., 1–[proportion of "low confidence" responses]) were calculated in order to evaluate the type 2 response bias (Fig. 4*c*). A two-way rmANOVA combining the two tasks was used for the statistical analysis (factors: stimulation site and task).

The proportions of "same" responses were calculated for evaluation of the type 1 response bias (see Supplementary Fig. S3). An equivalent analysis could have been performed using only the "different" responses. A two-way rmANOVA was used for the statistical analysis (factors: stimulation site and task).

Normality was tested using the Shapiro–Wilk test; all other behavioral data, except the response times data of two conditions (MFG site: temporal WM task, low confidence; control site: spatial WM task, high confidence), passed the test. The rmANOVAs were followed by post hoc tests, where appropriate. For post hoc testing, Tukey's multiple comparison test was applied. A *P*-value of <0.05 was considered to represent a statistically significant difference. Data were visualized as box plots, showing the median, 25th and 75th percentile (boxes), and minima and maxima (whiskers). Plotting and statistical computing was performed with GraphPad Prism (GraphPad Software Inc.).

Results

Influence of TMS on Metacognitive Accuracy

We investigated whether TMS of the tractography-informed cortical targets in the SFG and MFG affects metacognitive accuracy. Vertex stimulation provided a control condition. We calculated the meta-*d*' – *d*' for each task- and stimulation site with a sampling-based bootstrap statistical analysis for the pooled data (Fleming et al. 2014; Maniscalco and Lau 2015).

TMS applied to the SFG enhanced metacognitive accuracy in the temporal WM task, as revealed by the bootstrap distributions (Fig. 3*a*). The bootstrapped 95% CI of the SFG site had no overlap with those of the MFG or control TMS sites (SFG: −0.30 to 0.74; MFG: −1.56 to −0.47; Control: −1.67 to −0.50). In the SFG stimulation condition, the 95% CI of the bootstrap distribution in the temporal WM task overlapped with a meta-*d*' – *d*' value of 0, implying a metacognitively optimal accuracy. In contrast, the effect of TMS of the MFG did not differ from that of the control site in the temporal WM task, and the 95% CIs were below value 0 indicating a suboptimal metacognitive accuracy.

In the spatial WM task, neither TMS of the SFG nor of the MFG significantly affected metacognitive accuracy when compared with the control TMS condition (Fig. 3*b*), as shown by the overlapping 95% CIs of the bootstrap distributions (SFG: −1.20 to −0.19; MFG: −0.70 to 0.30; Control: −1.17 to −0.09).

We also performed direct comparisons of the bootstrap distributions *across* the two WM tasks. In this analysis, we compared the distributions of each stimulation site between the two tasks (i.e., [bootstrap distribution of spatial WM task] – [bootstrap distribution of temporal WM task]). The resulting 95% CI in the control site (−0.35 to 1.28) overlapped with zero, indicating that there was no difference in metacognitive accuracy between the tasks when stimulating the control site. The corresponding 95% CI of the MFG (0.08 to 1.51) did not overlap with zero, suggesting that when stimulating the MFG, the metacognitive accuracy was better in the spatial compared with the temporal WM task. In the SFG, comparison of the distributions (i.e., [bootstrap distribution of spatial WM task] – [bootstrap distribution of temporal WM task]) resulted in the 95% CI (−1.60 to −0.21) that was below zero suggesting a better metacognitive accuracy in the temporal compared with the spatial WM task.

An additional analysis of the bootstrapped, response-specific meta-*d*' –*d*' distributions showed that the enhancement of metacognitive accuracy by stimulation of the SFG was most pronounced when subjects answered "same" (see Supplementary Material, Fig. S5 and Table S2). Another additional analysis of metacognitive accuracy with the HMeta-d also yielded a similar result as in Figure 3: an improvement of metacognitive accuracy by TMS of the SFG in the temporal WM task (see Supplementary Fig. S6 and Table S3).

Other Behavioral Analyses

For the task performance analysis, the responses were grouped according to the confidence ratings (Lee et al. 2013). Separate

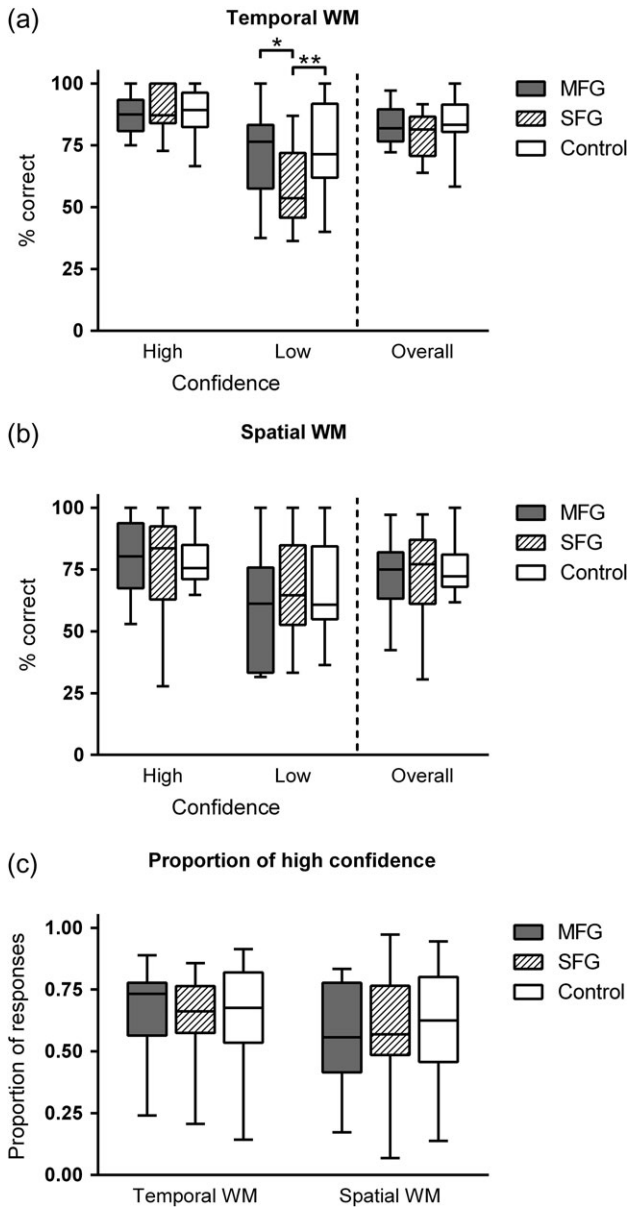

Figure 4. Effect of TMS on confidence ratings of responses. (*a*) In the temporal WM task, TMS of the SFG enhanced the matching of incorrectly performed trials with low confidence, whereas in the spatial WM task (*b*) the effect was absent. Overall performance is shown for illustrative purposes. (*c*) Average proportion of "high confidence" responses was unaffected by the tasks and different stimulation sites. Box plots show the median, lower, and upper quartiles (boxes), and minima and maxima (whiskers); $n = 14$; *$P < 0.05$, **$P < 0.01$ (Tukey's test).

two-way rmANOVAs were performed for the temporal and spatial WM tasks. The temporal WM performance was strongly associated with confidence ($F_{1,13} = 55.10$, $P < 0.0001$). The effect of the stimulation site was non-significant ($F_{2,26} = 2.49$, $P = 0.10$). Interestingly, there was a significant interaction of confidence and stimulation site in the temporal WM task ($F_{2,26} = 4.80$, $P = 0.017$). Post hoc analysis explained the observed effects; when TMS was applied to the SFG site in the temporal WM task, subjects rated incorrectly performed trials as low confidence trials more often than when TMS was applied to the control ($P = 0.0044$) or the MFG ($P = 0.012$; Fig. 4*a*) sites. All other post hoc comparisons in the temporal WM task were non-significant.

Analysis of the spatial WM task showed that the performance, again, was strongly associated with confidence ($F_{1,13} = 26.51$, $P = 0.0002$), but not with stimulation site ($F_{2,26} = 0.29$, $P = 0.75$; Fig. 4*b*). The interaction of confidence and stimulation site was non-significant ($F_{2,26} = 1.16$, $P = 0.33$).

To confirm that the results of the task performance and metacognitive accuracy analyses were not caused by shifts in type 2 response bias, we analyzed the proportion of "high confidence" responses across tasks and stimulation sites (Fig. 4*c*). A two-way rmANOVA showed that the effects of main factors (stimulation site: $F_{2,26} = 0.57$, $P = 0.57$; task: $F_{1,13} = 2.57$, $P = 0.13$) and their interaction (stimulation site × task: $F_{2,26} = 0.67$, $P = 0.52$) were not significant. Thus, the overall tendency of subjects to classify trials as "low confidence" or "high confidence" did not change across the tasks or stimulation sites. In the spatial WM task, the subjects responded "same" more often than in the temporal WM task, i.e., the two tasks had different type 1 response biases (see Supplementary Material, Fig. S3). Nevertheless, TMS did not affect the type 1 response bias within the tasks.

Furthermore, we checked whether the observed enhancement of metacognitive accuracy by TMS of the SFG in the temporal WM task could emerge from a difficulty difference between the two tasks. We compared the overall performances in the spatial and temporal tasks (*t*-tests with Bonferroni multiple comparisons correction). There were no significant differences in the difficulty level between the tasks at any of the TMS sites (MFG: $t_{13} = 2.31$, $P = 0.11$; SFG: $t_{13} = 0.69$, $P > 0.99$; control: $t_{13} = 2.52$, $P = 0.077$). The response times did not vary with TMS site (see Supplementary Material, Fig. S4).

Taken together, our results indicate that in the temporal WM task, TMS of the SFG caused subjects to assign their confidence rating more in line with their actual performance. Although it may seem counterintuitive, it is logical that the enhancement of the metacognitive accuracy is manifested as coupling of incorrect responses with low confidence rating; the subjects were more aware of their performance level in the incorrectly performed trials.

Discussion

In the current study, we demonstrate that single-pulse, tractography-guided TMS of a distinct prefrontal target improves metacognitive accuracy in a tactile WM task. We found that TMS of the SFG enhanced metacognitive accuracy of the temporal but not spatial WM, suggesting that metacognition is not a general phenomenon, but rather a specific, fine-tuned executive function with distinct neural substrates. Under the applied experimental conditions, TMS did not affect the overall WM performance indicating that TMS of the SFG affected specifically the metacognition of the temporal WM task. Moreover, the proportion of high and low confidence ratings did not change across tasks or stimulation sites. This indicates that the tendency of the subjects to classify trials as "low confidence" or "high confidence" did not change, but they could better match the incorrectly performed trials with low confidence.

The neural mechanism underlying the TMS-induced metacognitive improvement, observed in the current study, remains to be examined in the future. One possibility is that the TMS of the SFG enhanced metacognitive performance by a top-down control mechanism. The PFC has been shown to modulate WM by gating distractive noise and thus affecting information processing of more posterior cortical areas (Postle 2005). The PFC is

also known to control, amongst others, the alpha and gamma rhythms of the primary sensory areas (for a review, see Ku et al. 2015). Similar neurophysiological control mechanisms may explain a recent MEG result (Whitmarsh et al. 2017) in which a negative correlation was reported between alpha power in the left superior frontal area and metacognitive judgments of somatosensory attention. Interestingly, the peak voxel coordinates of the superior frontal area cluster (x −12, y 24, z 62) in the study by Whitmarsh et al. (2017) were close to the coordinates of the mean SFG_{HS} location (x −12, y 10, z 61) of our study.

Earlier TMS studies of our group have demonstrated the involvement of the MFG in tactile WM (Hannula et al. 2010; Savolainen et al. 2011) and tactile temporal perception (Gogulski et al. 2015). The finding of the current study that stimulation of the SFG, but not of the MFG, improved metacognitive accuracy only in the temporal WM task, suggests parcellation of the neural substrates underlying metacognition. Thus, although especially the anterior parts of the PFC have been associated with metacognitive processing (Fleming et al. 2010; Rahnev et al. 2016), the PFC might possess several differentiated neural underpinnings for introspection. Using diffusion tensor imaging and tractography, Gong et al. (2009) showed that the dorsal SFG is one of the major hub nodes of the human cortical networks that, like other hub regions, handles information from multiple other cortical regions, and thereby is in a position to contribute to complex cognitive functions.

The analysis of the response-specific meta-*d'* – *d'* (see Supplementary Material, Fig. S5 and Table S2) supported the main result of the current study indicating that TMS of the SFG enhanced metacognitive accuracy in the temporal WM task (Fig. 3). Response-specific bootstrap distributions showed that this improvement was most evident when the subjects responded "same". A similar trend was observed in the "different" response category of the temporal WM task (see Supplementary Fig. S5c). In the "same" response category of the temporal WM task, the 95% CI of the SFG bootstrap distribution did not overlap with meta-*d'* – *d'* value 0 (see Supplementary Table S2). A meta-*d'* – *d'* -value 0 would indicate a metacognitively optimal accuracy, whereas a value >0 has previously been suggested to reflect criterion variability (Maniscalco and Lau 2012). A recent review (Fleming and Daw 2017) suggests that this kind of "hyper" metacognitive accuracy may be related to improved error detection of low confidence responses. This is in line with our observation that stimulation of the SFG improved the ability of the subjects to rate the incorrectly performed trials as "low confidence" (Fig. 4*a*). Interestingly, in earlier fMRI and EEG studies, medial PFC areas close to our SFG targets have been linked with error detection (for a review, see Ullsperger et al. 2014). The observed modulation of confidence in a tactile WM task by TMS of SFG complements a recent fMRI study using a tactile discrimination task (Hilgenstock et al. 2014) that linked increased dorsolateral PFC activity with an increase in postdecisional uncertainty. Our results are also in line with recent theories of WM and conscious awareness which hypothesize that, at least in the visual modality, the WM contents and introspective awareness of WM might have dissociable neural frameworks (Soto and Silvanto 2014).

The spatial and temporal tactile WM tasks of the current study were designed so that the tactile stimuli and their timing were identical in both tasks; only the instructions to perform the tasks were different. The performance of the two tasks did not differ from each other significantly. Despite these similarities, all psychophysical properties of the tasks were not identical. While the type 2 response bias did not differ between the TMS sites or tasks (Fig. 4c), the type 1 response bias was different between the tasks (see Supplementary Material, Fig. S3). However, the meta-*d'* metric has been shown to be independent of type 1 response bias (Barrett et al. 2013; Maniscalco and Lau 2014).

Given the relatively low number of trials, the most preferable, subject-per-subject analysis of metacognitive accuracy would have yielded unstable estimates of meta-*d'* (Barrett et al. 2013). Thus, although not ideal, the data pooling and bootstrapping were reasonable approaches for the current study. To confirm that the metacognitive improvement in the temporal WM by TMS of the SFG was not caused by our calculation method, we applied a recently developed, hierarchical Bayesian calculation method (Fleming 2017) named HMeta-d (see Supplementary Fig. S6 and Table S3). HMeta-d – results were in line with the bootstrap results shown in Figure 3; in the temporal WM task, stimulation of the SFG enhanced metacognitive accuracy when compared with stimulation of the MFG or control site, whereas in the spatial WM task, the 95% CIs of all 3 stimulation sites overlapped. Moreover, in the SFG stimulation condition, the 95% CIs of the bootstrap distributions reflecting metacognitive accuracy did not overlap between the two tasks.

The main aim of the present study was to identify neural correlates underlying metacognitive accuracy in tactile WM. To accomplish this, we pursued to overcome problems related to interindividual differences in the topography of brain structure and function that may bias results of brain imaging studies relying on averaged group data. We first determined the cortical representation area of the tip of the index finger in each subject by blocking the tactile sensation with navigated TMS to the S1 cortex. We then determined, in each individual, the neural connections between this somatotopic representation area in the S1 cortex and the PFC by using probabilistic tractography. Furthermore, instead of relying on correlational associations between the function of a brain area and behavior, we applied navigated TMS to the tractography-informed areas of the PFC to build a causal link between the brain structure and behavioral function. With this approach we were able to show that TMS of the left tractography-informed SFG area enhanced metacognitive accuracy of tactile temporal but not spatial WM. The results are in accordance with earlier literature indicating that the PFC plays an important role in introspective judgements, and with a recent study that linked the left SFG with metacognitive ratings of somatosensory attention (Whitmarsh et al. 2017). Our results extend understanding of the neural mechanisms underlying WM and metacognition by providing causal evidence that the ability to monitor the WM performance may have distinct neural correlates in the PFC. The study also underlines the importance of taking individual functional anatomy into account in the experiments.

Supplementary Material

Supplementary data is available at *Cerebral Cortex* online.

Funding

The study was funded by the Sigrid Jusélius Foundation, the Academy of Finland (Grants # 259752, # 273147 and # 137795), Instrumentarium Science Foundation and Finnish Cultural Foundation.

Notes

We thank Jaana Hiltunen for advice concerning the diffusion-weighted MRI data acquisition. *Conflict of Interest*: None declared.

References

Andersson JL, Skare S, Ashburner J. 2003. How to correct susceptibility distortions in spin-echo echo-planar images: application to diffusion tensor imaging. Neuroimage. 20: 870–888.

Andersson JL, Sotiropoulos SN. 2016. An integrated approach to correction for off-resonance effects and subject movement in diffusion MR imaging. Neuroimage. 125:1063–1078.

Baddeley A. 1992. Working memory. Science. 255:556–559.

Barrett AB, Dienes Z, Seth AK. 2013. Measures of metacognition on signal-detection theoretic models. Psychol Methods. 18: 535–552.

Behrens T, Berg HJ, Jbabdi S, Rushworth M, Woolrich M. 2007. Probabilistic diffusion tractography with multiple fibre orientations: what can we gain? Neuroimage. 34:144–155.

Behrens T, Woolrich M, Jenkinson M, Johansen-Berg H, Nunes R, Clare S, Matthews P, Brady J, Smith S. 2003. Characterization and propagation of uncertainty in diffusion-weighted MR imaging. Magn Reson Med. 50:1077–1088.

Budisavljevic S, Dell'Acqua F, Zanatto D, Begliomini C, Miotto D, Motta R, Castiello U. 2016. Asymmetry and structure of the fronto-parietal networks underlie visuomotor processing in humans. Cereb Cortex. 27:1532–1544. doi:10.1093/cercor/bhv1348.

Chua EF, Pergolizzi D, Weintraub RR. 2014. The cognitive neuroscience of metamemory monitoring: understanding metamemory processes, subjective levels expressed, and metacognitive accuracy. In: Fleming SM, Frith CD, editors. The cognitive neuroscience of metacognition. New York: Springer. p. 267–291.

D'Esposito M, Postle BR. 2015. The cognitive neuroscience of working memory. Annu Rev Psychol. 66:115–142.

David AS, Bedford N, Wiffen B, Gilleen J. 2012. Failures of metacognition and lack of insight in neuropsychiatric disorders. Philos Trans R Soc Lond B Biol Sci. 367:1379–1390.

Fleming SM. 2017. HMeta-d: hierarchical Bayesian estimation of metacognitive efficiency from confidence ratings. Neurosci Conscious. doi:10.1093/nc/nix007.

Fleming SM, Daw ND. 2017. Self-evaluation of decision-making: a general Bayesian framework for metacognitive computation. Psychol Rev. 124:91–114.

Fleming SM, Dolan RJ. 2012. The neural basis of metacognitive ability. Philos Trans R Soc Lond B Biol Sci. 367:1338–1349.

Fleming SM, Lau HC. 2014. How to measure metacognition. Front Hum Neurosci. doi:10.3389/fnhum.2014.0044.

Fleming SM, Maniscalco B, Ko Y, Amendi N, Ro T, Lau H. 2015. Action-specific disruption of perceptual confidence. Psychol Sci. 26:89–98.

Fleming SM, Ryu J, Golfinos JG, Blackmon KE. 2014. Domain-specific impairment in metacognitive accuracy following anterior prefrontal lesions. Brain. 137:2811–2822.

Fleming SM, Weil RS, Nagy Z, Dolan RJ, Rees G. 2010. Relating introspective accuracy to individual differences in brain structure. Science. 329:1541–1543.

Gogulski J, Boldt R, Savolainen P, Guzman-Lopez J, Carlson S, Pertovaara A. 2015. A segregated neural pathway for prefrontal top-down control of tactile discrimination. Cereb Cortex. 25:161–166.

Goldman-Rakic P. 1995. Cellular basis of working memory. Neuron. 14:477–485.

Golestani AM, Miles L, Babb J, Castellanos FX, Malaspina D, Lazar M. 2014. Constrained by our connections: white matter's key role in interindividual variability in visual working memory capacity. J Neurosci. 34:14913–14918.

Gong G, He Y, Concha L, Lebel C, Gross DW, Evans AC, Beaulieu C. 2009. Mapping anatomical connectivity patterns of human cerebral cortex using in vivo diffusion tensor imaging tractography. Cereb Cortex. 19:524–536.

Gruber O, Kleinschmidt A, Binkofski F, Steinmetz H, Von Cramon DY. 2000. Cerebral correlates of working memory for temporal information. Neuroreport. 11:1689–1693.

Hannula H, Neuvonen T, Savolainen P, Hiltunen J, Ma YY, Antila H, Salonen O, Carlson S, Pertovaara A. 2010. Increasing top-down suppression from prefrontal cortex facilitates tactile working memory. Neuroimage. 49: 1091–1098.

Hannula H, Ylioja S, Pertovaara A, Korvenoja A, Ruohonen J, Ilmoniemi RJ, Carlson S. 2005. Somatotopic blocking of sensation with navigated transcranial magnetic stimulation of the primary somatosensory cortex. Hum Brain Mapp. 26: 100–109.

Hernández M, Guerrero GD, Cecilia JM, García JM, Inuggi A, Jbabdi S, Behrens TE, Sotiropoulos SN. 2013. Accelerating fibre orientation estimation from diffusion weighted magnetic resonance imaging using GPUs. PLoS One. doi:10.1371/journal.pone.0130915.

Hilgenstock R, Weiss T, Witte OW. 2014. You'd better think twice: post-decision perceptual confidence. Neuroimage. 99: 323–331.

Jenkinson M, Beckmann CF, Behrens TE, Woolrich MW, Smith SM. 2012. Fsl. Neuroimage. 62:782–790.

Kaas AL, Van Mier H, Goebel R. 2007. The neural correlates of human working memory for haptically explored object orientations. Cereb Cortex. 17:1637–1649.

Kanai R, Rees G. 2011. The structural basis of inter-individual differences in human behaviour and cognition. Nat Rev Neurosci. 12:231–242.

Kostopoulos P, Albanese M-C, Petrides M. 2007. Ventrolateral prefrontal cortex and tactile memory disambiguation in the human brain. Proc Natl Acad Sci USA. 104:10223–10228.

Ku Y, Bodner M, Zhou Y-D. 2015. Prefrontal cortex and sensory cortices during working memory: quantity and quality. Neurosci Bull. 31:175–182.

Lee TG, Blumenfeld RS, D'Esposito M. 2013. Disruption of dorsolateral but not ventrolateral prefrontal cortex improves unconscious perceptual memories. J Neurosci. 33:13233–13237.

Maniscalco B, Lau H. 2012. A signal detection theoretic approach for estimating metacognitive sensitivity from confidence ratings. Conscious Cogn. 21:422–430.

Maniscalco B, Lau H. 2014. Signal detection theory analysis of type 1 and type 2 data: meta-d′, response-specific meta-d′, and the unequal variance SDT model. In: Fleming SM, Frith CD, editors. The cognitive neuroscience of metacognition. New York: Springer. p. 25–66.

Maniscalco B, Lau H. 2015. Manipulation of working memory contents selectively impairs metacognitive sensitivity in a concurrent visual discrimination task. Neurosci Conscious. doi:10.1093/nc/niv002.

Mooney CZ, Duval RD. 1993. Bootstrapping: a nonparametric approach to statistical inference. Newbury Park (CA): Sage.

Mueller S, Wang D, Fox Michael D, Yeo BTT, Sepulcre J, Sabuncu Mert R, Shafee R, Lu J, Liu H. 2013. Individual

variability in functional connectivity architecture of the human brain. Neuron. 77:586–595.

Nelson TO, Narens L. 1990. Metamemory: a theoretical framework and new findings. Psychol Learn Motiv. 26:125–141.

Numminen J, Schürmann M, Hiltunen J, Joensuu R, Jousmäki V, Koskinen SK, Salmelin R, Hari R. 2004. Cortical activation during a spatiotemporal tactile comparison task. Neuroimage. 22:815–821.

Overgaard M. 2015. Behavioral methods in consciousness research. New York: Oxford University Press.

Penfield W, Boldrey E. 1937. Somatic motor and sensory representation in the cerebral cortex of man as studied by electrical stimulation. Brain. 60:389–443.

Petrides M. 2005. Lateral prefrontal cortex: architectonic and functional organization. Philos Trans R Soc Lond B Biol Sci. 360:781–795.

Pleger B, Ruff CC, Blankenburg F, Bestmann S, Wiech K, Stephan KE, Capilla A, Friston KJ, Dolan RJ. 2006. Neural coding of tactile decisions in the human prefrontal cortex. J Neurosci. 26:12596–12601.

Postle BR. 2005. Delay-period activity in the prefrontal cortex: one function is sensory gating. J Cognitive Neurosci. 17: 1679–1690.

Preuschhof C, Heekeren HR, Taskin B, Schubert T, Villringer A. 2006. Neural correlates of vibrotactile working memory in the human brain. J Neurosci. 26:13231–13239.

Preuss TM, Goldman-Rakic PS. 1989. Connections of the ventral granular frontal cortex of macaques with perisylvian premotor and somatosensory areas: anatomical evidence for somatic representation in primate frontal association cortex. J Comp Neurol. 282:293–316.

Rahnev D, Nee DE, Riddle J, Larson AS, D'Esposito M. 2016. Causal evidence for frontal cortex organization for perceptual decision making. Proc Natl Acad Sci USA. 113: 6059–6064.

Romanski LM, Tian B, Fritz J, Mishkin M, Goldman-Rakic PS, Rauschecker JP. 1999. Dual streams of auditory afferents target multiple domains in the primate prefrontal cortex. Nat Neurosci. 2:1131–1136.

Romo R, Brody CD, Hernández A, Lemus L. 1999. Neuronal correlates of parametric working memory in the prefrontal cortex. Nature. 399:470–473.

Romo R, Salinas E. 2003. Flutter discrimination: neural codes, perception, memory and decision making. Nat Rev Neurosci. 4:203–218.

Rounis E, Maniscalco B, Rothwell JC, Passingham RE, Lau H. 2010. Theta-burst transcranial magnetic stimulation to the prefrontal cortex impairs metacognitive visual awareness. Cogn Neurosci. 1:165–175.

Savolainen P, Carlson S, Boldt R, Neuvonen T, Hannula H, Hiltunen J, Salonen O, Ma YY, Pertovaara A. 2011. Facilitation of tactile working memory by top-down suppression from prefrontal to primary somatosensory cortex during sensory interference. Behav Brain Res. 219:387–390.

Smith SM, Jenkinson M, Woolrich MW, Beckmann CF, Behrens TE, Johansen-Berg H, Bannister PR, De Luca M, Drobnjak I, Flitney DE. 2004. Advances in functional and structural MR image analysis and implementation as FSL. Neuroimage. 23: S208–S219.

Soto D, Silvanto J. 2014. Reappraising the relationship between working memory and conscious awareness. Trends Cogn Sci. 18:520–525.

Stoeckel MC, Weder B, Binkofski F, Buccino G, Shah NJ, Seitz RJ. 2003. A fronto-parietal circuit for tactile object discrimination: An event-related fMRI study. Neuroimage. 19: 1103–1114.

Ullsperger M, Danielmeier C, Jocham G. 2014. Neurophysiology of performance monitoring and adaptive behavior. Physiol Rev. 94:35–79.

Whitmarsh S, Barendregt H, Schoffelen J-M, Jensen O. 2014. Metacognitive awareness of covert somatosensory attention corresponds to contralateral alpha power. Neuroimage. 85: 803–809.

Whitmarsh S, Oostenveld R, Almeida R, Lundqvist D. 2017. Metacognition of attention during tactile discrimination. Neuroimage. 147:121–129.

Wilson F, Scalaidhe S, Goldman-Rakic P. 1993. Dissociation of object and spatial processing domains in primate prefrontal cortex. Science. 260:1955–1958.

Woolrich MW, Jbabdi S, Patenaude B, Chappell M, Makni S, Behrens T, Beckmann C, Jenkinson M, Smith SM. 2009. Bayesian analysis of neuroimaging data in FSL. Neuroimage. 45:S173–S186.

Yokoyama O, Miura N, Watanabe J, Takemoto A, Uchida S, Sugiura M, Horie K, Sato S, Kawashima R, Nakamura K. 2010. Right frontopolar cortex activity correlates with reliability of retrospective rating of confidence in short-term recognition memory performance. Neurosci Res. 68:199–206.

Zilles K, Schleicher A, Langemann C, Amunts K, Morosan P, Palomero-Gallagher N, Schormann T, Mohlberg H, Burgel U, Steinmetz H, et al. 1997. Quantitative analysis of sulci in the human cerebral cortex: development, regional heterogeneity, gender difference, asymmetry, intersubject variability and cortical architecture. Hum Brain Mapp. 5:218–221.